



## Treatment of oil-in-water emulsion using tubular ceramic membrane acquired from locally available low-cost inorganic precursors

R. Vinoth Kumar<sup>a</sup>, P. Monash<sup>b</sup>, G. Pugazhenthii<sup>a,\*</sup>

<sup>a</sup>Department of Chemical Engineering, Indian Institute of Technology Guwahati, Guwahati 781039, Assam, India, email: [vinoth@iitg.ernet.in](mailto:vinoth@iitg.ernet.in) (R. Vinoth Kumar), Tel. +91 361 2582264; Fax: +91 361 2582291; email: [pugal@iitg.ernet.in](mailto:pugal@iitg.ernet.in) (G. Pugazhenthii)

<sup>b</sup>Department of Chemical Engineering, University of Malaya, Kuala Lumpur 50603, Malaysia, email: [monash@um.edu.my](mailto:monash@um.edu.my)

Received 1 October 2015; Accepted 10 April 2016

---

### ABSTRACT

This article highlights the fabrication of ceramic membrane with tubular configuration using locally available inexpensive clays and its application in oil-in-water emulsion treatment. Extrusion technique was employed to manufacture the tubular-shaped ceramic membrane having length, outer, and inner diameters of 100, 12, and 6.5 mm, respectively. Clay powders and the fabricated membrane were characterized using standard techniques such as particle size distribution, scanning electron microscopy, energy dispersive X-ray spectroscopy, X-ray diffraction, thermogravimetric (TG), and field emission scanning electron microscopy analysis. The fabricated membrane possessed porosity of 50%, average pore diameter of 0.339  $\mu\text{m}$ , and mechanical strength of 12 MPa with relatively good corrosion resistance in acidic and basic conditions. The effect of various operating conditions such as pressure (69–345 kPa) and cross-flow velocity (0.044–0.132 m/s) on the microfiltration process of oil-in-water emulsion was studied using this membrane with a fixed feed oil concentration of 100 mg/L in a cross flow manner. The research findings indicated that the rejection of oil slightly decreased with the rise in pressure. The best rejection of 99.88% was obtained with permeate flux of  $3.40 \times 10^{-5} \text{ m}^3/\text{m}^2 \text{ s}$  at an applied pressure of 68 kPa after 1 h of experimental run. These results demonstrated the application of the fabricated membrane in oil-in-water emulsion treatment and the treated water can be directly discharged into water bodies. Finally, the estimation of the manufacturing cost of the acquired membrane was presented in detail.

*Keywords:* Cost estimation; Low-cost membrane; Oil-in-water emulsion; Tubular membrane; Wastewater treatment

---

### 1. Introduction

The swift developments of various industries specifically, oil refineries, petrochemical, metallurgical, pharmaceutical, chemical, and food industries, are

bearing to produce a huge amount of both water-in-oil or oil-in-water emulsions. These contain bulk quantity of heavy hydrocarbons such as diesel oil, grease, crude oils, tars, and light hydrocarbons, such as gasoline, jet fuel, and kerosene. In addition, these comprise cutting liquids, lubricants, total suspended solid, and other supplemental contaminants [1,2]. The discharge

---

\*Corresponding author.

of oil-contaminated effluents to water bodies generate environmental issues all over the globe. Concurrently, the population growth directs to the bigger demand for pure water, primarily in water scarcity regions [3]. Therefore, the removal of oil from the oily wastewater is necessary to protect our water resources in both environmental and public health. Central pollution control board of India regulated the discharge limit of oil into the surface water and irrigation as 10 mg/L, public sewers and coastal water as 20 mg/L from various process industries [4]. Beside the treatment, the stable oily wastewater containing extremely physically and chemically emulsified oils are the major difficult ones in terms of efficient treatment [5]. The conventional techniques utilized in water treatment plants to treat the wastewater can be classified as creational: chemical demulsification, gravity separation, adsorption, filtration, coagulation, and coalescence [6]. These techniques have various demerits including higher operation expenses, lower effectiveness, corrosion and recontamination issues [7]. One of the best solutions to resolve these problems and reuse water is using membrane technology. Currently, industries have paid increasing attention for the membrane technology [8].

In the membrane separation process, inorganic membranes have been proven to be well suitable and more favorable for large-scale applications compared to the organic (polymeric) membranes. Inorganic membranes have higher chemical, thermal, and mechanical resistance and can be used in the wide range of pH, chlorinated, and polar solvents [9]. However, the alumina-based inorganic membranes are unfavorable to large-scale industrial applications due to its high cost. Therefore, the research on ceramic membrane is directed to make low-cost membranes by utilizing cheaper starting materials, such as kaolin, mullite, fly ash, apatite powder, and dolomite [10]. In this context, manufacturing reasonably inexpensive inorganic membranes for oil-in-water emulsion treatment is potentially useful for future membrane development research. In addition, membranes come in four different configurations, including tubular, hollow fiber, plate and frame, and spiral. Tubular membranes are suitable for handling large size particles and high flow rates, and they can be cleaned easily [11]. Therefore, the low-cost membrane with tubular configuration is well suitable particularly for oil-in-water emulsion treatment.

To the best of our knowledge, the following studies have approached to fabricate the tubular configuration membranes using inexpensive raw materials for oily wastewater treatment. Abbasi et al. [5] synthesized tubular mullite microfiltration membrane from

kaolin clay, which was obtained from Marand, Iran. The tubular-shaped mullite membrane was suitably acquired through extrusion using 62–69% of kaolin and distilled water mixture. The potential of the fabricated membrane was investigated by the separation of oil-in-water emulsion and the influences of various significant conditions, namely pressure (50–400 kPa), cross-flow velocity (0–2 m/s), and oil concentration (250–3,000 ppm) were also examined. The investigation on oil-in-water emulsion treatment revealed that the prepared membrane has potential to get the highest rejection of 93.8%. Fang et al. [12] elaborated new fly ash-based low-cost membrane for treatment of oily wastewater. Macroporous fly ash-based ceramic membrane was obtained by an extrusion process. The acquired membrane tested for microfiltration of oily wastewater by varying the operating parameters, such as transmembrane pressure (0.05–0.20 MPa), feed concentration (75–2,000 ppm), and cross-flow velocity (0.67–4 m/s). The highest rejection (98.2%) of oil was obtained with the feed concentration of 2,000 ppm. Song et al. [13] prepared the low-cost tubular carbon membrane using coal via extrusion technique and used for oil-in-water emulsion treatment. This investigation was performed by altering various parameters, such as membrane pore size (0.6–1.4  $\mu\text{m}$ ), transmembrane pressure (60–140 kPa), feed oil concentration (120–400 ppm), and cross-flow velocity (0.06–10 m/s). The maximum rejection of 98.6% was obtained with the feed concentration of 400 ppm. It is worth mentioning that all these investigations were performed using higher concentration of oil-in-water emulsion at elevated cross-flow velocities. The treatment of low concentration ( $\leq 100$  ppm) oily wastewater to the disposal limit (10–20 ppm) is difficult by most of the conventional separation techniques [14]. Secondly, a higher cross-flow velocity directs to superior energy requirements to pump the feed stock and thus the selection of higher cross-flow velocities is not favorable in economical point of view.

Considering the above limitations, we made an effort to make low-cost tubular configuration membrane using locally available low-cost inorganic precursors. The essential characterizations of raw materials are deeply discussed and efficiency of the fabricated membrane is examined by oil-in-water emulsion treatment. Microfiltration experiments operated at different controlling parameters, such as pressure and cross-flow velocity are investigated using a feed oil concentration of 100 ppm. Also, the manufacturing cost of the fabricated membrane is estimated in the preliminary economic evaluation at research level.

## 2. Experimental

### 2.1. Materials

The locally available low-cost inorganic precursors of mineral grade were used for the preparation of the membrane (ball clay, feldspar, kaolin, pyrophyllite and quartz). Hydrochloric acid, calcium carbonate, and sodium hydroxide were supplied by Merck (I) Ltd, Mumbai.

### 2.2. Membrane preparation

An extrusion process was adopted to form a tubular-shaped membrane. The table top hand extruder (M/s VB Ceramic Consultants, Chennai, India) made of stainless steel was used for obtaining tubular ceramic tubes. It essentially consists of a feed chamber, extruder screw shafts, cone, and die assemblies. The green dough was prepared from the mixture of clays, calcium carbonate and Millipore water without the addition of any organic chemicals for plasticity. Calcium carbonate powder was used as a pore-former agent. In our previous work [15], we reported the preparation of circular-shaped ceramic membranes using these clay mixtures and the optimum composition of clay powders was selected based on the superior properties (such as porosity, pore size, mechanical, and chemical stability) of the membrane. In this work also, the identical (optimum) composition of clay powders were used for the fabrication of tubular membrane as follows: Ball clay—18 wt%, Feldspar—6 wt%, Kaolin—15 wt%, Pyrophyllite—15 wt%, Quartz—28 wt%, and Calcium carbonate—18 wt%. The procedure for the fabrication of membrane is diagrammatically presented in Fig. 1. The feedstock was shaped into tubes using die assemblies with length, inner, and outer diameters of 100, 6.5, and 12 mm, respectively, at room temperature. The extruded green tube was subjected to controlled thermal treatment by employing the following procedure to avoid uneven shrinkage upon drying and subsequent deformation during sintering. The obtained green tubular membrane was firstly placed for natural drying at atmospheric condition for 24 h. After which, the membrane was dried at 200 °C for 24 h in a hot air oven. Subsequently, the membrane was taken to the sintering process at 950 °C with a heating rate of 2 °C/min and kept at this temperature for 6 h in a box furnace. To attain a homogeneous even surface, the fabricated inflexible and porous sintered tubular membrane was burnished and sized using dry abrasive grinding sandpaper. To remove the unsticking powders formed through burnishing and sizing activities, the membrane was treated with water in an ultrasonic

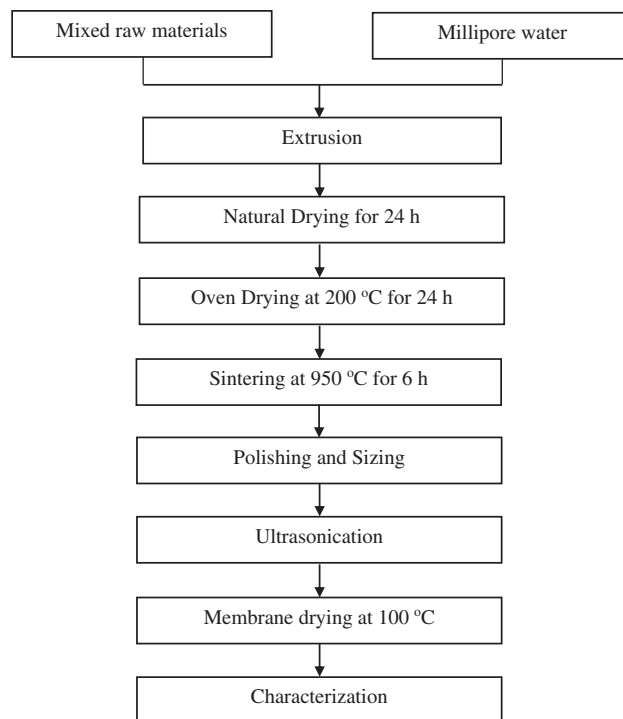


Fig. 1. Schematic representation of tubular ceramic membrane fabrication.

bath (Elma T460, India) for 30 min. Finally, the membrane was dried at 100 °C and utilized for further characterization.

### 2.3. Characterization methods

#### 2.3.1. Raw materials

The particle size distribution (PSD) of raw materials was analyzed in Malvern Mastersizer 2000 (APA5005<sup>®</sup> model, hydro MU) instrument in wet dispersion mode by circulating the heterogeneous feed at constant flow rate (pump speed = 2,700 rpm) with an ultrasound to avoid the agglomeration of clay powders during analysis. Scanning electron microscopy (SEM) investigations were conducted in a varying pressure digital SEM (LEO1430VP<sup>®</sup>) combined with an energy dispersive X-ray spectroscope. The X-ray diffraction (XRD) profiles recorded with Cu K $\alpha$  ( $\lambda = 1.5406 \text{ \AA}$ ) radiation working at 40 kV and 40 mA in a Bruker AXS machine in  $2\theta$  value ranging between 5° and 75° with a scan rate of 0.05°/s. Mettler Toledo (TGA/SDTA 851<sup>®</sup>) thermogravimetric instrument (NETZSCH TG 209F1 Libra) was used to characterize the thermal decomposition activities of the clay powders in air atmosphere with a heating rate of 10 °C/min from 25 to 970 °C in a 150  $\mu\text{L}$  platinum container.

### 2.3.2. Tubular ceramic membrane

The tubular membrane was characterized by field emission scanning electron microscopy (FESEM) (JEOL, JSM-5600LV) to analyze the presence of possible defects on the surfaces. A small size of the membrane sample was fixed on top of the stub and layered with gold using an auto fine coating instrument (JEOL JFC-1300) preceding morphology assessment. The porosity of the membrane was determined by liquid displacement method using Millipore water [16]. Resistance in corrosion capability of the fabricated membrane was investigated by means of loss of mass after treating in high corrosive environments. The extreme harsh condition solutions, such as HCl (pH 1) and NaOH (pH 14) solutions, were prepared and the membrane was immersed in it for one week. The corrosion resistance of the recovered membrane was evaluated by weight decrement of the membrane. The flexural strength of the membrane was calculated by three-point bending method using Universal Testing Machine (M/s Deepak Polyplast, Model: DUTT-101, Mumbai) according to the procedure reported elsewhere [17].

### 2.4. Experimental setup and water flux measurement

In this work, the cross flow filtration system was employed for water flux measurement and microfiltration of oil-in-water emulsion. Fig. 2 illustrates the real picture representation of the experimental system, in which the entire experiments were performed. The system consists of feed tank, pump, membrane module, pressure gauge and three flow control valves in inlet, by-pass, and retentate flow paths. The experimental setup is easy to operate without complication, conversely, it made in such a manner that the essential significant working conditions for the microfiltration study, such as pressure and cross-flow velocity can be turned and fixed. During the microfiltration study, the process system was cautiously watched to maintain the desired pressure and cross-flow velocity.

Water flux was evaluated at different applied pressures as a function of time for a fixed cross-flow velocity. The water flux reaches steady value after some time of filtration. After attained stable flux, water flux was evaluated at diverse pressures (69–345 kPa) at a preset cross-flow velocity (0.088 m/s) for 15 min according to the following relation:

$$J_w \text{ (flux)} = \frac{Q \text{ (volume of water permeated, m}^3\text{)}}{A \text{ (area, m}^2\text{)} \times t \text{ (time, s)}} \quad (1)$$

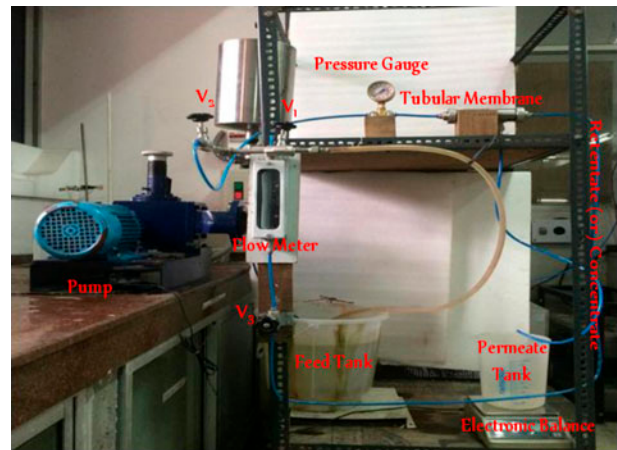


Fig. 2. Representation of experimental system.  
Notes:  $V_1$ —by-pass valve,  $V_2$ —inlet valve,  $V_3$ —retentate valve.

### 2.5. Filtration of oil-in-water emulsion and membrane regeneration

Synthetic oil-in-water emulsion was subjected to analyze the potential of the tubular ceramic microfiltration membrane. Crude oil collected from Guwahati Refinery, Indian Oil Corporation Limited (IOCL), India, was used without any treatment to prepare synthetic oil-water emulsions. The crude oil was obtained from Assam crude oil reservoirs. Assam crude is typically characterized to possess a high degree of aromatic and wax content [18]. The oil-in-water emulsion having a concentration of 100 ppm was made by crude oil emulsification in Millipore water with the following procedure: 1,000 mg of crude oil was dissolved in 10 liters of Millipore water and the suspension was subjected to ultrasonication for about 12 h. The emulsification process was carried out without the addition of any emulsifier agents. The droplet size of the emulsion in the feed was calculated by laser diffraction spectroscopy (Malvern Mastersizer, United Kingdom) and the mean droplet size is calculated to be 0.99  $\mu\text{m}$ . The cross flow microfiltration of oil-in-water emulsion was performed for a period of 1 h at various pressures (69–345 kPa) and cross-flow velocities (0.044–0.132 m/s). The concentration of oil was measured using ultraviolet-visible spectrophotometer (Thermo Scientific, UV-2300) at a wavelength of 236 nm and the rejection was calculated as follows:

$$R \text{ (rejection, \%)} = 1 - \frac{C_p \text{ (oil concentration in permeate)}}{C_f \text{ (oil concentration in feed)}} \times 100 \quad (2)$$

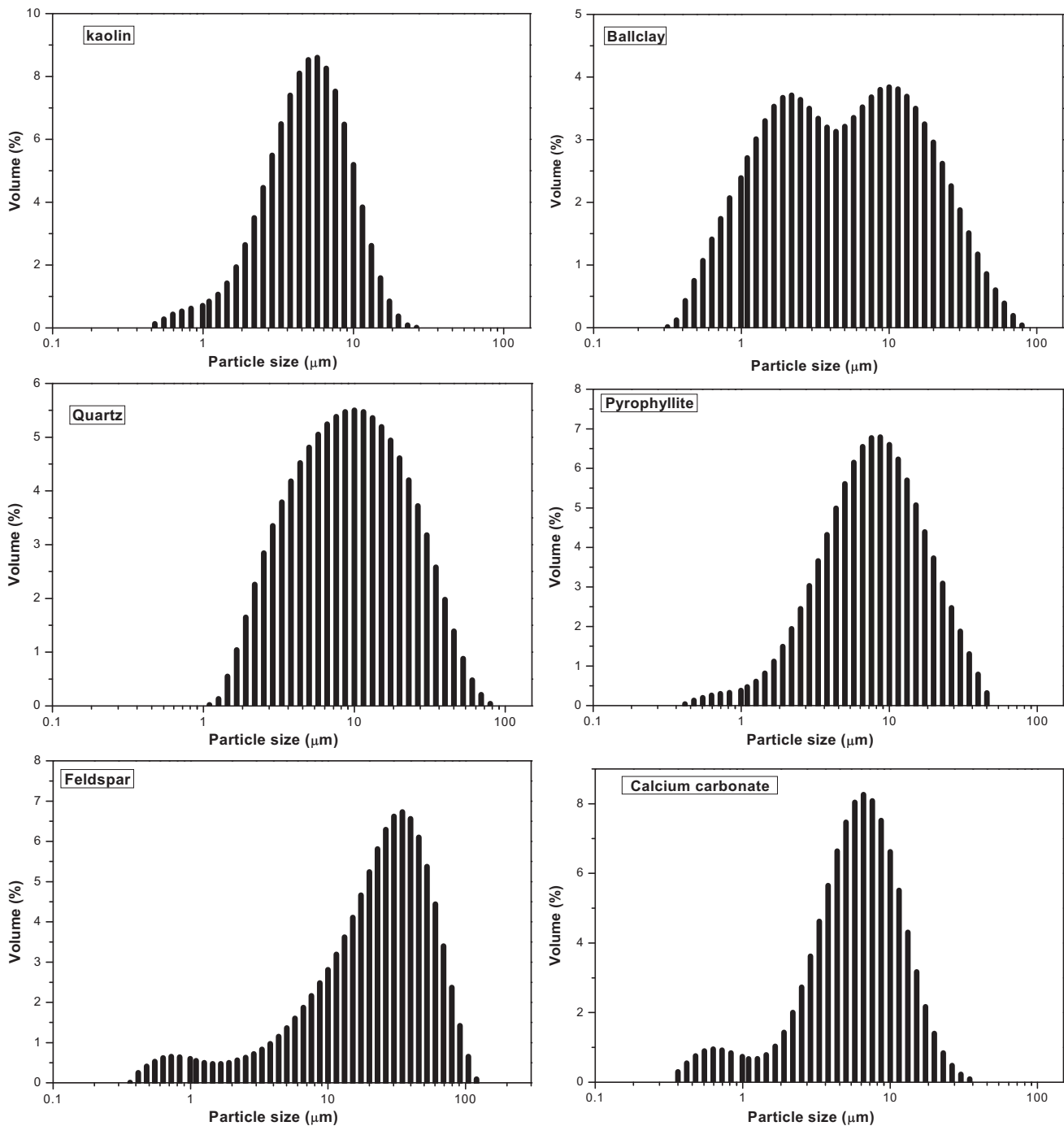


Fig. 3. PSD of the clay powders used for preparation of membrane.

The membrane was thoroughly cleaned and reused after each experimental run. For cleaning of the membrane, the following steps were adopted sequentially: firstly, the membrane was washed by passing the cleansing agent (commercially acquired surf-excel powder, 1 g/L) to the filtration system to eliminate the deposited oil on the surface of the membrane dur-

ing the filtration. After which, the whole system was cleaned by passing Millipore water. To verify the regeneration of the membrane, the water flux of the membrane was evaluated again after cleaning process and if the variation of water flux between the fresh membrane and cleaned membrane is less than 5%, then it can be taken for further experiments.

Table 1  
PSD of various clay powders used in the preparation of membrane

Clay powder	Particle size			Span	Specific surface area (m <sup>2</sup> /g)	D(2, 3) (μm)	D(4, 3) (μm)
	D(V, 0.1) (μm)	D(V, 0.5) (μm)	D(V, 0.9) (μm)				
Kaolin	1.852	04.656	9.814	1.710	1.750	3.419	05.354
Feldspar	3.855	22.925	56.284	2.287	0.315	6.898	27.082
Quartz	2.680	08.650	27.107	2.824	0.994	6.034	12.242
CaCO <sub>3</sub>	2.083	06.460	14.299	1.891	1.610	3.735	07.557
Ballclay	0.954	05.039	24.749	4.722	0.923	2.499	09.659
Pyrophyllite	2.805	08.428	22.786	2.371	0.379	5.581	10.926
Mixture	1.840	07.326	24.450	3.125	0.516	4.094	10.639

Notes: D(3, 2) = surface area moment mean or the Sauter Mean Diameter (SMD).

D(4, 3) = volume or mass moment mean or the De Broucker mean.

D(V, 0.5) = volume median diameter sometimes shown as D<sub>50</sub> or D<sub>0.5</sub>.

### 3. Results and discussion

#### 3.1. Characterization of clay powders

Sintering temperature and pore size of the ceramic membrane can be regulated by the particle size of raw materials used for membrane fabrication. The formation of pore on the ceramic membrane is a function of the initial particle size of the clay powders [19]. The finer particles require reasonably lower temperature for sintering; however, it leads to the resistance of a larger transport due to extremely small effectual pore size. Conversely, courser materials require relatively high sintering temperature, and it leads to the resistance of a small transport due to macropores, but the mechanical strength is reduced [20]. The PSDs of the individual clay powders are presented in Fig. 3. All the analysis is done two times for the laser obscuration limit greater than 10% and the average value of the results is presented in Table 1. The volume or mass moment mean, D(3, 4) and surface area moment mean, D(2, 3) are calculated using the following formula:

$$D(4, 3) = \frac{\sum d^4}{\sum d^3} \quad (3)$$

$$D(3, 2) = \frac{\sum d^3}{\sum d^2} \quad (4)$$

where  $d$  is the particle diameter (μm).

The advantage of this method of calculation (Eqs. (3) and (4)) is that formulae do not contain the number of particles and therefore the calculations of the means and distributions do not require knowledge of the number of particles involved. D(3, 4) is usually reported in a prominent manner.

The volume-weighted mean formula is utilized to evaluate the diameter of the clay particles and their

sizes vary between 5 and 10 μm. This range of particle size of clays is favorable to manufacture the ceramic membranes. Similar PSDs of clays were applied for the fabrication of macroporous membrane [21]. The surface area of the raw material in the increasing order is as follows: feldspar < pyrophyllite < ballclay < quartz < calcium carbonate < kaolin. This is also considered while choosing the composition of the raw materials for membrane preparation. This provides a knowledge regarding the composition of clays to be utilized for the fabrication of the membrane.

Span is also another valuable consideration in calculating the applicability of the clay mixture that can be evaluated using the following expression:

$$\text{Span} = \frac{D_{90} - D_{10}}{D_{50}} \quad (5)$$

A larger span value could be owing to one or more of the following: (a) very high  $D_{90}$  and very small  $D_{10}$ , (b) moderate  $D_{90}$  and  $D_{10}$ , but very small  $D_{50}$ . A higher span value with a very high  $D_{90}$  is unfavorable for the fabrication of ceramic membranes due to a higher percentage of coarser particles [20]. Span values attained from the study are calculated to be in the similar range (1.8–3) for all clays, which specifies an equivalent width of the size distributions. This offers a well mixing and homogeneous distribution between the particles that could result in a good microfiltration membrane.

Scanning electron microscope images of the clay powders along with the energy dispersive X-ray spectroscopy (EDX) are presented in Fig. 4. The EDX analysis (qualitative analysis) of kaolin, ball clay, and pyrophyllite indicates that the clay powders contain oxides of aluminum and silicon. However, no other

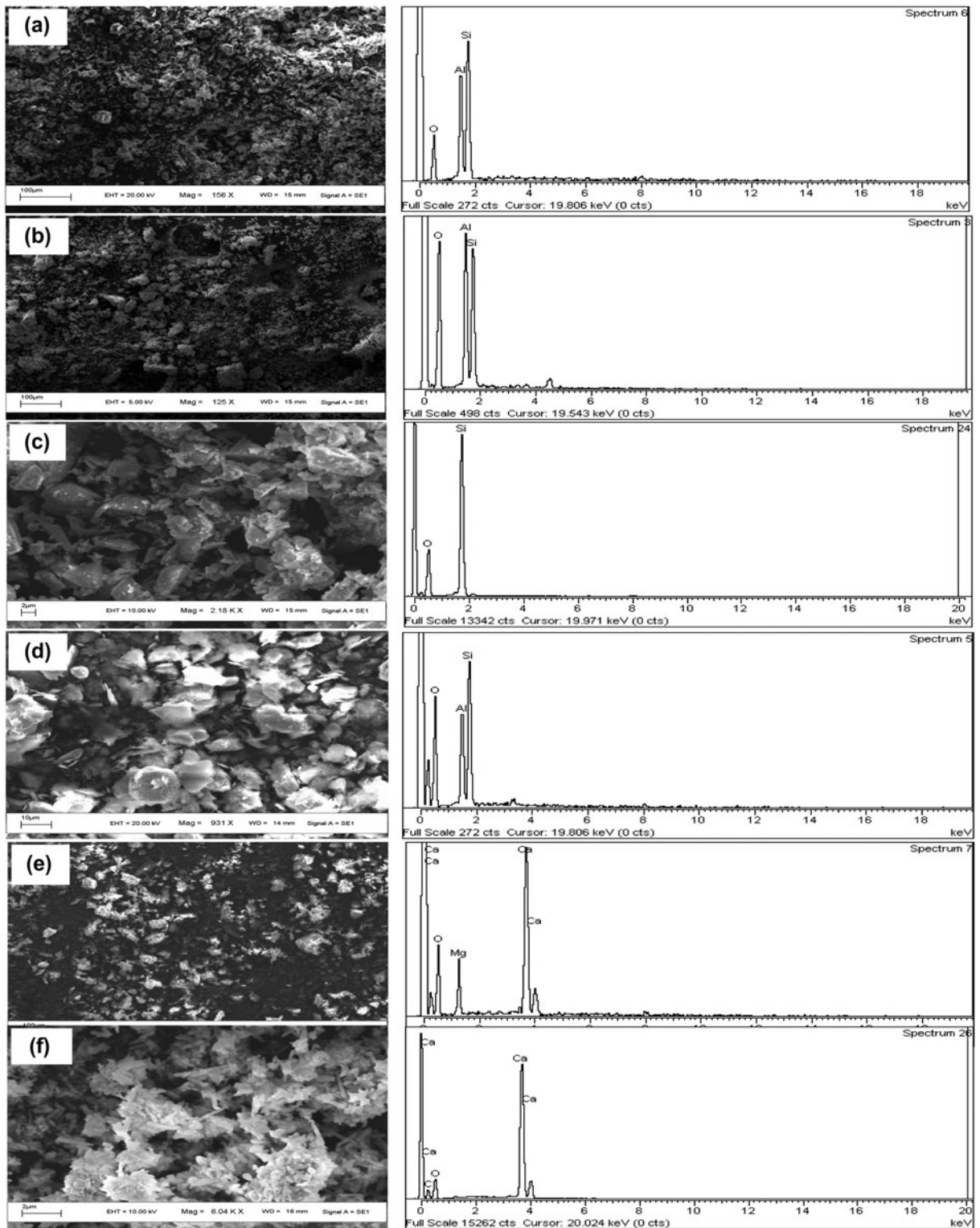


Fig. 4. SEM and EDX analysis of the clay powders used in membrane fabrication: (a) Kaolin, (b) Ball clay, (c) Quartz, (d) Pyrophyllite, (e) Feldspar, and (f) CaCO<sub>3</sub>.

peaks are obtained even using spot EDS at higher magnification, suggesting that it is free from other impurities or has only a trace amount of impurities (<5 wt%) that cannot be detected by SEM. Quartz shows only the oxides of silicon that indicates its purity. The elemental peak of Ca obtained for feldspar signifies that the feldspar is of plagioclase type, which is triclinic in nature. The commercially purchased calcium carbonate shows only the peaks of Ca and O,

which confirms its purity. The Si/Al ratio obtained with the EDX analysis of different clays is apparently closer to the theoretical value of those clays [22].

Similarly, all the clay powders were analyzed with XRD and the obtained patterns are well matching with the standard Joint Committee on Powder Diffraction Standards (JCPDS) files. The XRD patterns of the clay powders are presented in Fig. 5. The XRD peaks of the kaolin match well with the reflections of standard

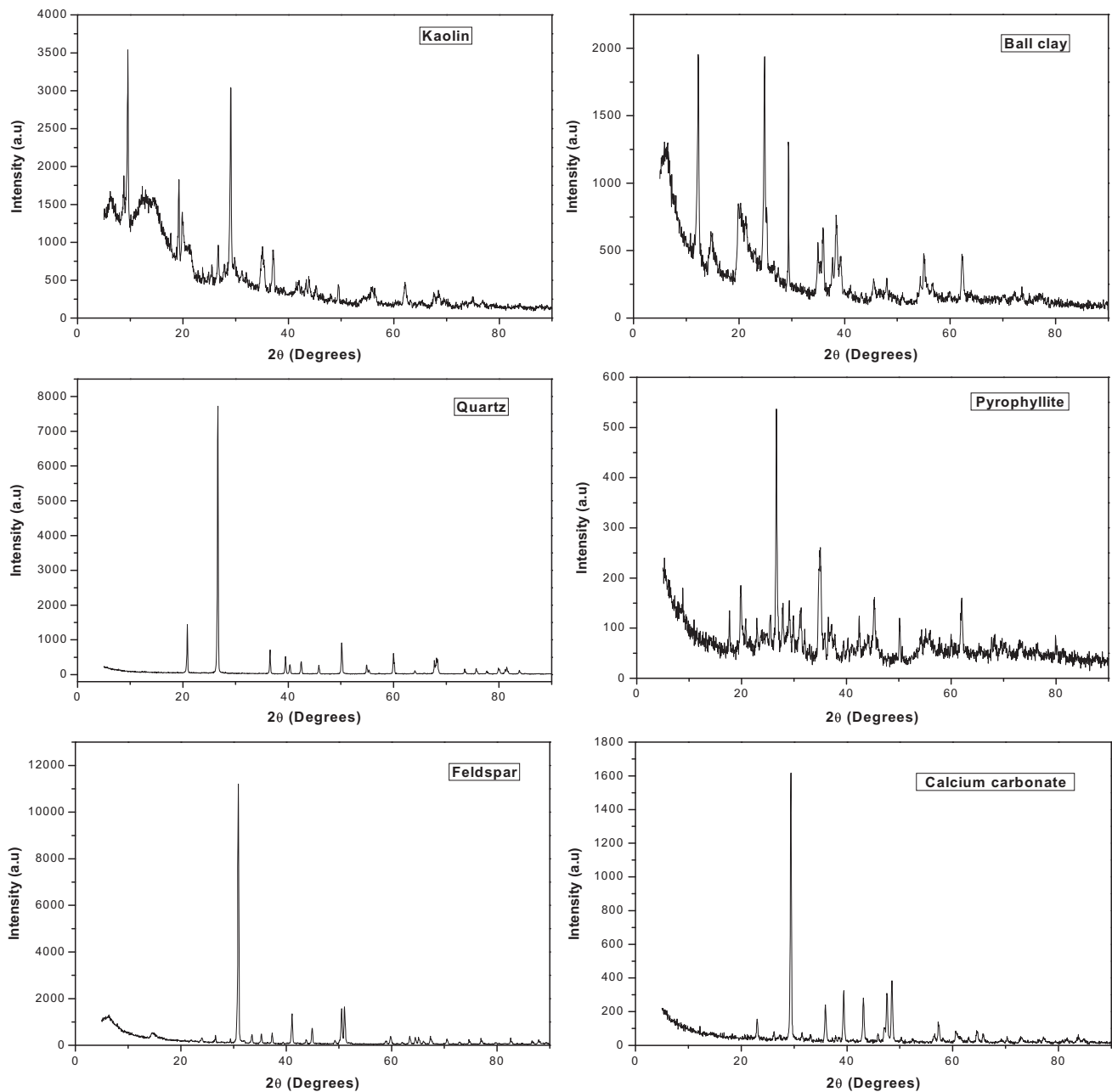


Fig. 5. XRD patterns of the clays used for the preparation of membrane.



JCPDS card number 14-164 and the other additional reflections match with the JCPDS card number 10-446. This indicates that kaolin also contains dickite, which is the same composition as kaolinite with different crystal structure [22]. The main crystalline phases observed in the ball clay corresponds to kaolin ( $2\theta = 12.25^\circ$  and  $24.85^\circ$ ) and quartz. The  $2\theta$  reflections ( $2\theta = 20.85^\circ$  and  $26.65^\circ$ ) of quartz match well with the JCPDS card number 46-1045, which corresponds to the pure quartz phase [23]. Similarly, the  $2\theta$  reflections of pyrophyllite and feldspar are in good agreement with the standard JCPDS card number 12-203 and 09-456, respectively [24].

Sintering temperature is an essential factor to control the mechanical strength, pore size, and porosity of the ceramic membrane. TGA of clay powders was done to discover the minimum sintering temperature required for the fabrication of stable membrane and the obtained results are plotted in Fig. 6. The weight decrement at temperature  $<150^\circ\text{C}$  is mainly owing to the elimination of physisorbed water and at higher temperature ( $500\text{--}800^\circ\text{C}$ ), the decrement is due to the dehydroxylation of the surface hydroxyl group or exclusion of structural water. Thermal decomposition ( $550\text{--}750^\circ\text{C}$ ) of  $\text{CaCO}_3$  results in major weight loss and forms  $\text{CaO}$  and  $\text{CO}_2$ . The porosity of the membrane primarily corresponds to the pathway occurred through the evolved  $\text{CO}_2$  gas. Due to the increased release of OH groups attached to Al and Si and subsequent conversion of kaolin to metakaolin, ball clay shows a relatively higher weight loss (14.11%) than that of kaolin (5.04%) and

pyrophyllite (9.70%). It can be seen that no significant weight decrement is observed after the temperature of  $820^\circ\text{C}$ . This points out that to acquire inflexibility membrane with good mechanical and thermal strength, the green membrane should be sintered above the temperature of  $850^\circ\text{C}$ . Mapping analysis of the SEM as shown in Fig. 7 validates the homogeneous distribution of silica-aluminates throughout the membrane. The elements identified by the EDX are Al and Si, which are in the form of oxides ( $\text{Al}_2\text{O}_3$  and  $\text{SiO}_2$ ). Ca is in the form of  $\text{CaO}$  as well as wollastonite and anorthite.

### 3.2. Characterization of ceramic membrane

FESEM images were used to analyze both inner and outer surface morphology of the fabricated membrane (see Fig. 8(a) and (b)). These figures give information on the consistency of the prepared membrane surfaces. It is found that the membrane is highly smooth with flawless inner and outer surfaces. The overall surface morphological analysis recommends that the non-appearance of cracks/defects/big pores is a key condition leading to a good quality membrane. The average porosity and flexural strength of the membrane are calculated to be 50% and 12 MPa, respectively. In the chemical stability investigation, the weight decrement of the membrane is evaluated to be 12% in acidic condition and 0% in alkali condition. This clearly signifies that the membrane has relatively good resistance in these solutions. It is worth to mention that cordierite membrane displayed the mass loss of 17.01% in acidic solution [25], which is higher than the current investigation.

Moreover, the variation of applied pressure on water flux has been studied. It is apparent from Fig. 9 that the water flux increases linearly with an increase in the pressure (69–345 kPa). This stipulates that the applied pressure is the barely driving force for permeation. For transportation operation exclusively by convection, the volumetric flow rate is proportionate to the pressure, which is an act in accordance with Darcy's law. The water permeability of the membrane is calculated as  $7.35 \times 10^{-7} \text{ m}^3/\text{m}^2 \text{ s kPa}$ . The average pore size was determined using porosity and water permeability values by Hagen–Poiseuille expression [16,26]. The mean pore size of the membrane is calculated to be  $0.339 \mu\text{m}$ . It can be concluded that the fabricated membrane could be applied for industrial utilization due to its excellent membrane characteristics such as mechanical strength, quality surface, porosity, pore size, corrosion resistance, and water permeability.

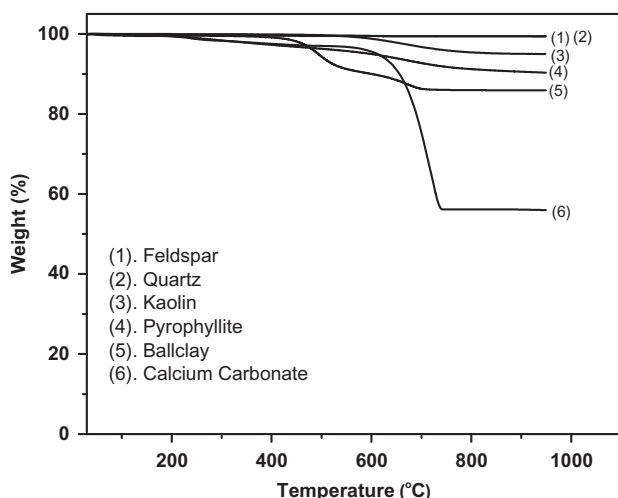


Fig. 6. TGA profiles of the clays used for the preparation of membrane.

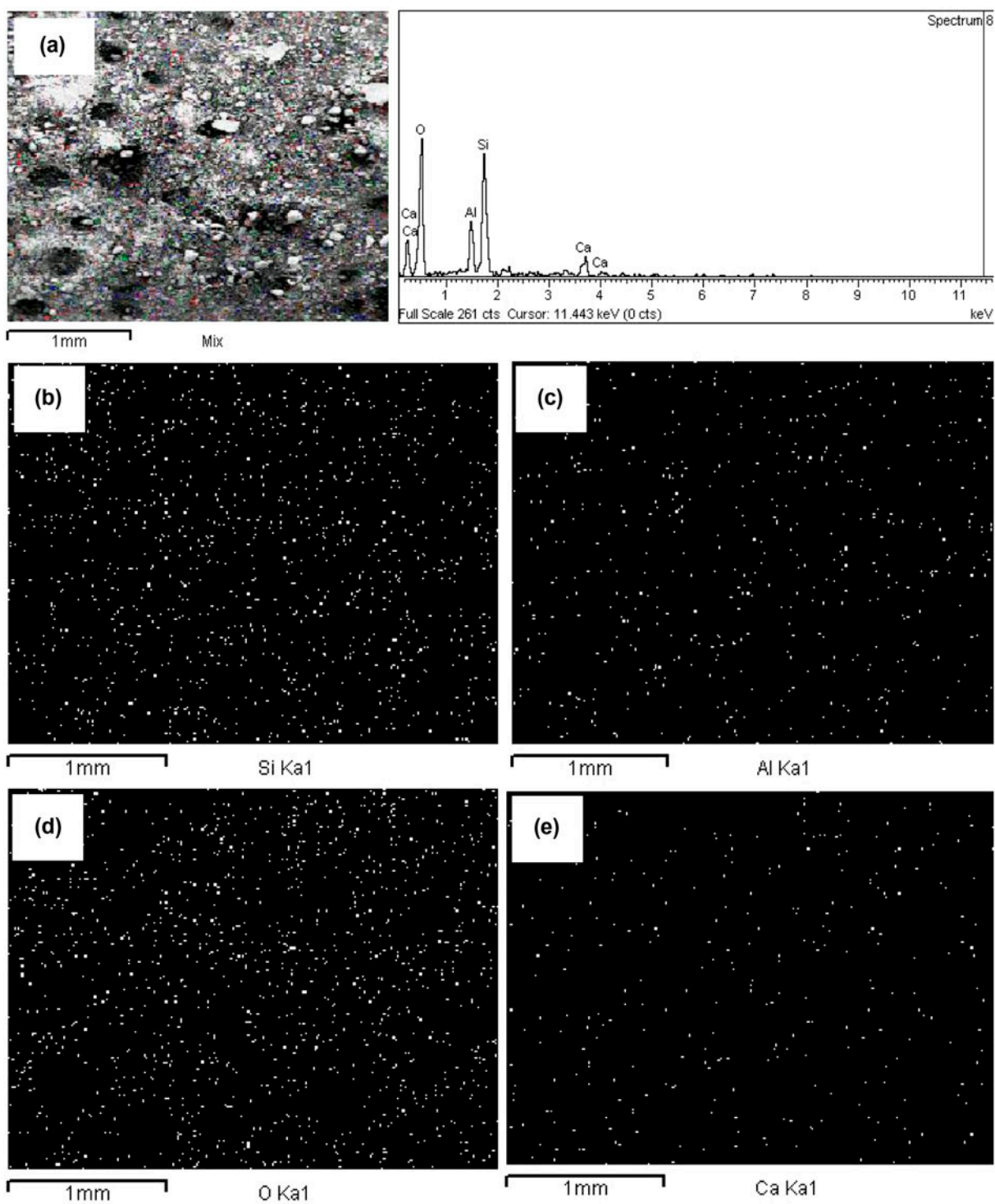


Fig. 7. SEM mapping analysis of the sintered membrane: (a) zone at which EDX and mapping analysis done, (b)–(e) represents the mapping results of Si, Al, O, and Ca, respectively.

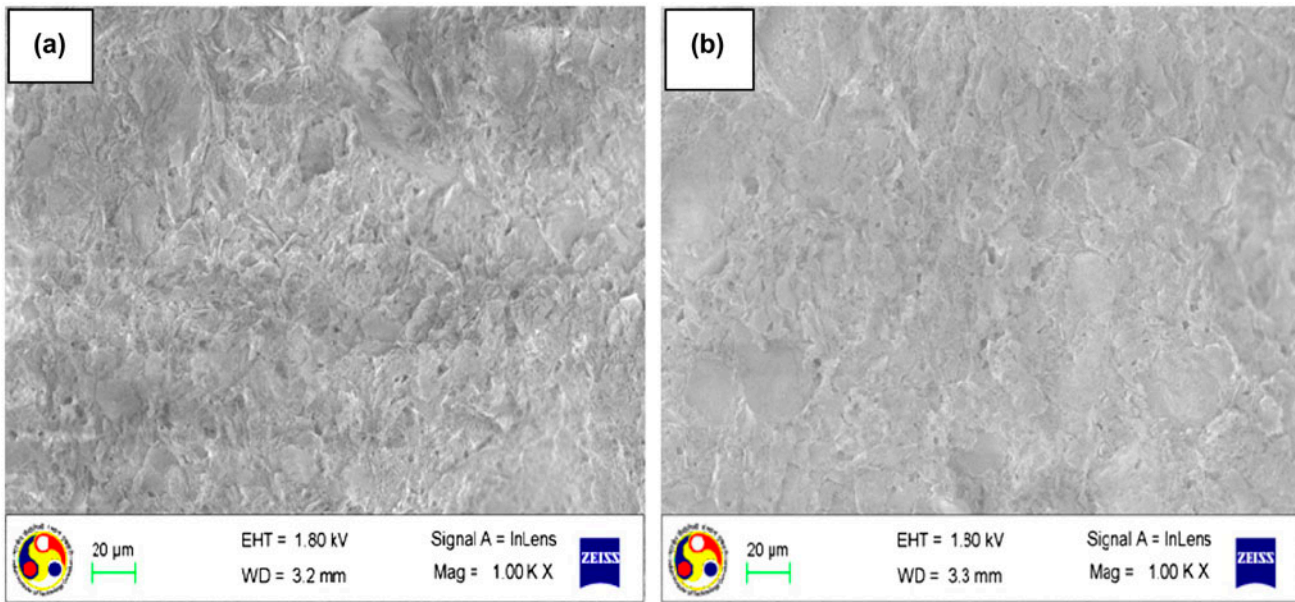


Fig. 8. FESEM images of (a) inner and (b) outer surfaces of the membrane.

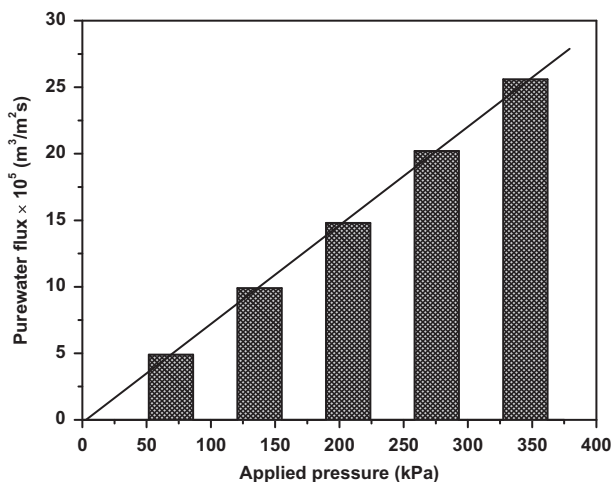


Fig. 9. Water flux vs. applied pressure.

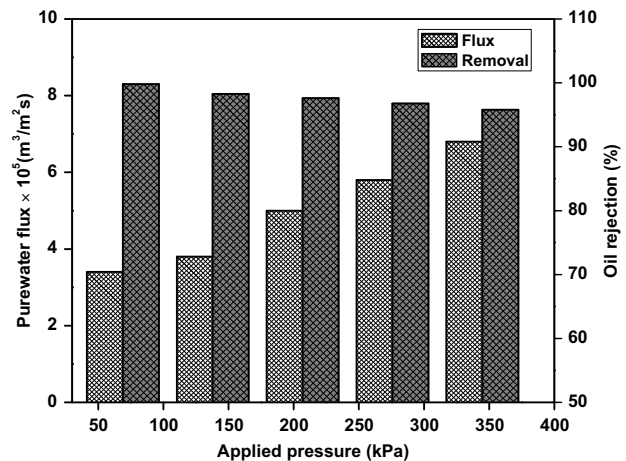


Fig.10. Effect of pressure on permeate flux and oil rejection in microfiltration process (cross-flow velocity = 0.088 m/s, concentration of oil = 100 ppm).

### 3.3. Treatment of oil-in-water emulsions by clay-based microfiltration membrane

#### 3.3.1. Effect of pressure on the microfiltration process

Fig. 10 illustrates the permeate flux and removal efficiency of oil after 60 min of experimental run with various pressures (69, 138, 207, 278, and 345 kPa) for a cross-flow velocity of 0.088 m/s. It is noticed that there is an augmentation in the flux when the pressure increases. This is owing to the enhanced driving force

across the membrane. However, the permeate flux of oil–water emulsion is lower than that of the corresponding water flux. According to Darcy's law, the permeate flux shows enhancement with increasing pressure; conversely, this fundamental law is restricted by fouling. Oil droplets closely packed on the surface of the membrane at elevated pressures offer to block the pores of the membrane. Moreover, it can be explained by concentration polarization and adsorption of oil on the surface, which creates further resistances to transport

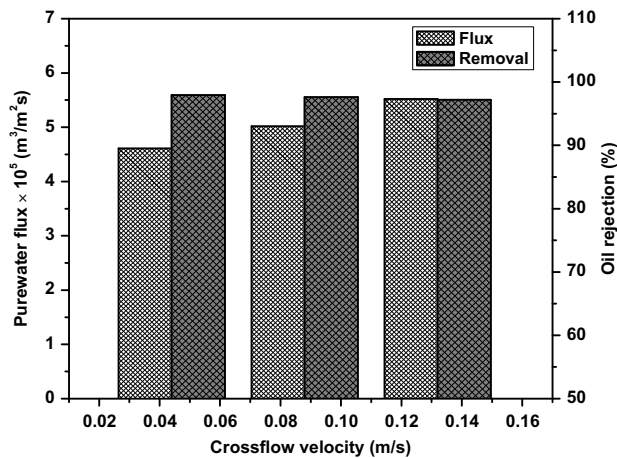


Fig. 11. Effect of cross-flow velocity on permeate flux and oil rejection in microfiltration process (pressure = 207 kPa, concentration of oil = 100 ppm).

liquid through the membrane [5]. The removal efficiency of oil-in-water emulsion declines with an increment in the pressure for a fixed concentration. This occurs due to the fact that the oil droplets deform at higher pressures and penetrates to the smaller pores, resulting in decrement in the removal [14]. In the effect of pressure study, the membrane exhibits the greatest rejection of 99.88% with permeate flux of  $3.40 \times 10^{-5} \text{ m}^3/\text{m}^2 \text{ s}$  at a lower applied pressure of 68 kPa.

### 3.3.2. Effect of cross-flow velocity on the microfiltration process

Fig. 11 illustrates the filtration flux and removal efficiency of oil-in-water emulsion after 60 min of experimental run with various cross-flow velocities (0.044, 0.088, and 0.132 m/s) for a fixed pressure of 207 kPa. The plot designates that the higher cross-flow velocity leads to offer a higher flux in the microfiltration due to decrement in the concentration polarization. Another reason is that the oil droplets get a little difficult to adsorb over the surface of the membrane at higher cross-flow velocity and the membrane fouling

resistance decreases with increasing flow velocity [27]. An enhancement in the cross-flow velocity eliminates the deposition of oil layer on the surface of the membrane, which results in reducing the oil removal slightly. In the study on the effect of cross-flow velocity, the highest oil rejection of 98.78% is obtained with lower cross-flow velocity of 0.044 m/s at an applied pressure of 207 kPa.

### 3.3.3. Performance evaluation of the membrane

The performance of the membrane in oil-in-water emulsion treatment is analyzed with other low-cost membranes prepared, particularly in the tubular configuration and utilized for oily wastewater treatment. The prepared membrane exhibits the highest rejection of 99.88% at an applied pressure of 68 kPa with the feed concentration of 100 mg/L and cross-flow velocity of 0.088 m/s. From Table 2, it can be seen that attempted studies on treatment of oily wastewater using the low-cost tubular membrane is carried out with higher concentration and elevated cross-flow velocities. As discussed, the treatment of oily wastewater containing lower concentration is difficult and higher cross-flow velocity directs to superior energy requirements to pump the feed stock. Thus, the selection of higher cross-flow velocities is not favorable in economical point of view. This study is attempted with a lower concentration of oil-in-water emulsion and low cross-flow velocity and the attained highest rejection is compared to those reported in literature. In few words, the prepared tubular ceramic membrane demonstrates to be the best in comparison with other membranes in terms of rejection and economical point of view.

### 3.4. Estimation of manufacturing cost of the membrane

A detailed analysis on manufacturing cost of the membrane is calculated and presented in Table 3. The manufacturing cost is estimated in the preliminary economic evaluation at research level [28]. The manufacturing cost is the sum of all the direct costs and

Table 2  
Performance evaluation of prepared membrane with other low-cost membranes

Membrane material	Oil concentration (mg/L)	Cross-flow velocity (m/s)	Rejection (%)	Refs.
Mullite	1,000	1.50	93.8	[5]
Fly ash	2,000	4.00	98.2	[12]
Carbon	400	0.10	98.6	[13]
Clays	100	0.08	99.8	Present study

Table 3  
Estimation of manufacturing cost of the membrane

Items	Calculation basis for making hundred membranes				US\$
	Raw materials	Unit price (US\$/kg)	Materials utilized (g)	Cost (US\$)	
Direct manufacturing costs: raw materials					
	Kaolin	0.18	142.8	0.03	
	Quartz	0.30	262.8	0.08	
	CaCO <sub>3</sub>	5.40	169.4	0.92	
	Ball clay	0.09	173.7	0.02	
	Phyrophyllite	0.15	145.6	0.02	
	Feldspar	0.12	055.3	0.01	
			Total cost for raw materials:		1.08
Labor (including supervisory)	Labor cost = cost × total hours = 2.81 × 8				22.48
Electricity	Furnace: 12.25 h × 4 kW = 49 kW; 54.83 kW × US\$ 0.09 = 4.93				
	Hot air oven: 30 h × 3 kW = 90 kW 90 × US\$ 0.09 = 8.10				
	Ultrasonicator: 0.5 h × 2 kW = 1 kW 1 × US\$ 0.09 = 0.09				
	Extruder: 1 kW/HP × 0.5 HP × 1.40 h 0.7 kW × US\$ 0.09 = 0.06				
			Total electricity cost		13.18
Maintenance	Maintenance cost = (capital cost × 1%)/d				
	Extruder = 1,500				
	Hot air oven = 600				
	Furnace = 2,250				
	Ultrasonicator = 375				
	Capital cost = 4,725				
			Total maintenance cost:		0.13
Laboratory	Laboratory cost = 20% of labor cost				
			Laboratory cost:		4.50
Indirect manufacturing costs: capital cost	Calculated by straight line method, $d = \frac{V-V_s}{n}$ where $d$ —annual depreciation cost, $V$ —original cost, $V_s$ —Salvage cost, $n$ —service life				0.50
Total manufacturing costs	direct manufacturing costs + indirect manufacturing costs				41.87
Estimated manufacturing cost for one membrane					0.4187
Estimated manufacturing cost for one membrane (round off value): US\$ 0.5					

indirect costs of the actual manufacturing cost of the product. The direct manufacturing cost of the membrane includes the costs of raw materials, labor, electricity, maintenance, and laboratory. The raw material cost is estimated by consumption of raw materials to prepare the membrane. Labor cost is calculated by the use of a correlation of labor in a man-hour per day. The maintenance cost is estimated as 1% of the capital cost and laboratory cost is estimated as 20% of the labor cost [28]. The indirect manufacturing cost (capital cost), counting with the depreciation cost is

calculated by straight line method. The manufacturing cost of the prepared tubular ceramic membrane is estimated to be 0.5 \$/membrane (or 69 \$/m<sup>2</sup>). Therefore, it can be concluded from the estimated manufacturing cost, the prepared membrane is very inexpensive.

#### 4. Conclusions

The low-cost tubular microfiltration membrane is prepared by locally available cheaper materials. The raw materials and membrane were characterized by

PSD, SEM, EDX, XRD, thermogravimetric (TG), and FESEM analysis. The efficiency of the fabricated membrane is examined by oil-in-water emulsion treatment at various pressures and cross-flow velocity, which have observable changes on permeate flux and rejection. The rejection declines with an increment in pressures and the high cross-flow velocity enhances the flux and decreases the rejection. The membrane exhibits the highest rejection of 99.88% at an applied pressure of 68 kPa with lower cross-flow velocity. The obtained rejection value meets the specification given by the central pollution control board of India for oily wastewater. Moreover, the prepared tubular ceramic membrane displays the best results as compared to other tubular membranes reported in the literature in terms of both rejection and cost. Finally, the manufacturing cost of the membrane estimated to be 0.5 \$/membrane. Overall study concludes that this inexpensive microfiltration membrane could be applied for oil-in-water emulsion treatment.

### Acknowledgment

We would like to thank the Central Instruments Facility at IIT Guwahati for helping us to perform FESEM analysis.

### List of symbols

$J_w$	—	flux ( $\text{m}^3 \text{m}^{-2} \text{s}^{-1}$ )
$Q$	—	volume of permeated water ( $\text{m}^3$ )
$A$	—	area ( $\text{m}^2$ )
$t$	—	time (s)
$C_f$	—	concentration in feed ( $\text{mg L}^{-1}$ )
$C_p$	—	concentration in permeate ( $\text{mg L}^{-1}$ )
$R$	—	rejection (%)
$d$	—	particle diameter ( $\mu\text{m}$ )
\$	—	United States dollar

### References

- [1] M. Padaki, R.S. Murali, M. Abdullah, N. Misdan, A. Moslehyani, M. Kassim, Membrane technology enhancement in oil–water separation. A review, *Desalination* 357 (2015) 197–207.
- [2] A. Salahi, T. Mohammadi, R. Mosayebi Behbahani, M. Hemmati, Asymmetric polyethersulfone ultrafiltration membranes for oily wastewater treatment: Synthesis, characterization, ANFIS modeling, and performance, *J. Environ. Chem. Eng.* 3 (2015) 170–178.
- [3] A. Salahi, I. Noshadi, R. Badrnezhad, B. Kanjilal, T. Mohammadi, Nano-porous membrane process for oily wastewater treatment: Optimization using response surface methodology, *J. Environ. Chem. Eng.* 1 (2013) 218–225.
- [4] Central Pollution Control Board (CPCB), India, 2014. Available from: <[http://www.cpcb.nic.in/Industry\\_Specific\\_Standards.php](http://www.cpcb.nic.in/Industry_Specific_Standards.php)>.
- [5] M. Abbasi, M. Mirfendereski, M. Nikbakht, M. Golshenas, T. Mohammadi, Performance study of mullite and mullite-alumina ceramic MF membranes for oily wastewaters treatment, *Desalination* 259 (2010) 169–178.
- [6] P. Srijaroonrat, E. Julien, Y. Aurelle, Unstable secondary oil/water emulsion treatment using ultrafiltration: Fouling control by backflushing, *J. Membr. Sci.* 159 (1999) 11–20.
- [7] A. Rezvanpour, R. Roostaazad, M. Hesampour, M. Nyström, C. Ghotbi, Effective factors in the treatment of kerosene-water emulsion by using UF membranes, *J. Hazard. Mater.* 161 (2009) 1216–1224.
- [8] M.V. Sarfaraz, E. Ahmadpour, A. Salahi, F. Rekabdar, B. Mirza, Experimental investigation and modeling hybrid nano-porous membrane process for industrial oily wastewater treatment, *Chem. Eng. Res. Des.* 90 (2012) 1642–1651.
- [9] B.K. Nandi, A. Moparathi, R. Uppaluri, M.K. Purkait, Treatment of oily wastewater using low cost ceramic membrane: Comparative assessment of pore blocking and artificial neural network models, *Chem. Eng. Res. Des.* 88 (2010) 881–892.
- [10] M. Karhu, T. Kuokkanen, J. Rämö, M. Mikola, J. Tanskanen, Performance of a commercial industrial-scale UF-based process for treatment of oily wastewaters, *J. Environ. Manage.* 128 (2013) 413–420.
- [11] M. Cheryan, *Ultrafiltration and Microfiltration Handbook*, CRC Press, Florida, 1998.
- [12] J. Fang, G. Qin, W. Wei, X. Zhao, L. Jiang, Elaboration of new ceramic membrane from spherical fly ash for microfiltration of rigid particle suspension and oil-in-water emulsion, *Desalination* 311 (2013) 113–126.
- [13] C. Song, T. Wang, Y. Pan, J. Qiu, Preparation of coal-based microfiltration carbon membrane and application in oily wastewater treatment, *Sep. Purif. Technol.* 51 (2006) 80–84.
- [14] P. Monash, G. Pugazhenth, Effect of  $\text{TiO}_2$  addition on the fabrication of ceramic membrane supports: A study on the separation of oil droplets and bovine serum albumin (BSA) from its solution, *Desalination* 279 (2011) 104–114.
- [15] P. Monash, G. Pugazhenth, Development of ceramic supports derived from low-cost raw materials for membrane applications and its optimization based on sintering temperature, *Int. J. Appl. Ceram. Technol.* 8 (1) (2011) 227–238.
- [16] R.V. Kumar, A.K. Basumatary, A.K. Ghoshal, G. Pugazhenth, Performance assessment of an analcime-C zeolite-ceramic composite membrane by removal of Cr(VI) from aqueous solution, *RSC Adv.* 5 (2015) 6246–6254.
- [17] O. David, Y. Gendel, M. Wessling, Tubular macro-porous titanium membranes, *J. Membr. Sci.* 461 (2014) 139–145.
- [18] V.C. Kandwal, K.M. Agrawal, S.P. Nautiyal, H.U. Khan, Paraffin deposition and viscosity temperature behaviour of Assam crude oil, *Pet. Sci. Technol.* 18 (2000) 755–769.
- [19] M. Fukushima, Y. Zhou, Y.I. Yoshizawa, Fabrication and microstructural characterization of porous SiC membrane supports with  $\text{Al}_2\text{O}_3$ - $\text{Y}_2\text{O}_3$  additives, *J. Membr. Sci.* 339 (2009) 78–84.

- [20] Y.H. Wang, Y. Zhang, X.Q. Liu, G.Y. Meng, Sol-coated preparation and characterization of macroporous  $\alpha$ -Al<sub>2</sub>O<sub>3</sub> membrane support, *J. Sol-Gel. Sci. Technol.* 41 (2007) 267–275.
- [21] M. Almandoz, J. Marchese, P. Prádanos, L. Palacio, A. Hernández, Preparation and characterization of non-supported microfiltration membranes from aluminosilicates, *J. Membr. Sci.* 241 (2004) 95–103.
- [22] M. Castellano, A. Turturro, P. Riani, T. Montanari, E. Finocchio, G. Ramis, G. Busca, Bulk and surface properties of commercial kaolins, *Appl. Clay Sci.* 48 (2010) 446–454.
- [23] J. González, A. Carreras, M.D.C. Ruiz, Phase transformations in clays and kaolins produced by thermal treatment in chlorine and air atmospheres, *Latin Am. Appl. Res.* 37 (2007) 133–139.
- [24] K. Sugiyama, H. Ryu, Y. Waseda, Local ordering structure of meta-kaolinite and meta-dickite by the X-ray radial distribution function analysis, *J. Mater. Sci.* 28 (1993) 2783–2788.
- [25] Y. Dong, X. Feng, D. Dong, S. Wang, J. Yang, J. Gao, X. Liu, G. Meng, Elaboration and chemical corrosion resistance of tubular macro-porous cordierite ceramic membrane supports, *J. Membr. Sci.* 304 (2007) 65–75.
- [26] R.V. Kumar, A.K. Ghoshal, G. Pugazhenth, Fabrication of zirconia composite membrane by in-situ hydrothermal technique and its application in separation of methyl orange, *Ecotoxicol. Environ. Saf.* 121 (2015) 73–79.
- [27] Y.-R. Qiu, H. Zhong, Q.-X. Zhang, Treatment of stable oil/water emulsion by novel felt-metal supported PVA composite hydrophilic membrane using cross flow ultrafiltration, *Trans. Nonferrous Met. Soc. China* 19 (2009) 773–777.
- [28] O. Winter, Preliminary economic evaluation of chemical processes at the research level, *Ind. Eng. Chem.* 61 (1969) 45–52.